The mechanobiology of tendon fibroblasts under static and uniaxial cyclic load in a 3D tissue engineered model mimicking native ECM

Prasad Sawadkar[1*], Darren Player[1], Laurent Bozec[2] and Vivek Mudera[1]

1 Division of Surgery and interventional Science, UCL Stanmore campus, London, UK
2 Biomaterials and Tissue Engineering, UCL Eastman Dental Institute, London, UK

.

*To whom correspondence should be addressed:

Dr Prasad Sawadkar
Division of Surgery and interventional Science,
University College London, Stanmore campus,
London HA7 4LP
United Kingdom
E mail- prasad.sawadkar@ucl.ac.uk
Phone- (+44) 020- 89542300
Fax (+44) 020 89548560

ABSTRACT

Tendon mechanobiology plays a vital role in tendon repair and regeneration; however, this mechanism is currently poorly understood. We tested the role of different mechanical loads on extra-cellular matrix (ECM) remodelling gene expression and the morphology of tendon fibroblasts in collagen hydrogels, designed to mimic native tissue. Hydrogels were subjected to precise static or uniaxial loading patterns of known magnitudes and sampled to analyse gene expression of known mechano-responsive ECM-associated genes (COL I, COL III, Tenomodulin and TGF-β). Tendon fibroblast cytomechanics was studied under load by using a tension culture force monitor (t-CFM), with immunofluorescence and immunohistological staining used to examine cell morphology. Tendon fibroblasts subjected to cyclic load showed endogenous matrix tension was maintained, with significant concomitant upregulation of ECM remodelling genes, COL I, COL III, Tenomodulin, and TGF-b when compared to static load and control samples. These data indicate that tendon fibroblasts acutely adapt to the mechanical forces placed upon them, transmitting forces across the ECM without losing mechanical dynamism. This model demonstrates cell-material (ECM) interaction and remodelling in pre-clinical a platform, which can be used as a screening tool to understand tendon regeneration.

1. INTRODUCTION

The primary function of the tendon is to transmit the force generated by the muscles to the bones, required to initiate movement and skeletal stability. Thus, the tendon is always under intrinsic tension, which makes them more prone to injuries (Y. Liu, Ramanath, & Wang, 2008; Murchison et al., 2007)

Tendons display a distinct ability to alter their physical and mechanical functions, depending on the stress placed upon them. This dynamic mechanical adaptation plays a vital role in tendon healing and regeneration (Killian, Cavinatto, Galatz, & Thomopoulos, 2012; Thomopoulos, 2011; J. H. Wang, Guo, & Li, 2012). Specialised residing fibroblasts, called simply tendon fibroblasts (TF), are thought to regulate mechanical homeostasis through altering extra-cellular matrix (ECM) turnover. This mechanism increases tensile strength and the cross-linked area of the tendon but is currently poorly understood (Killian et al., 2012; J. H. Wang, 2006). It is thought that mechanical forces also lead to cytoskeletal deformation, which triggers the onset of biochemical signalling and cellular alignment in the tissue. Indeed, it has been demonstrated that cellular deformation in the tendon is an indication that TF adapts to the mechanical force (Arnoczky, Lavagnino, Whallon, & Hoonjan, 2002). Furthermore, TF can sense mechanical stress placed upon them, increasing the production of ECM remodelling genes such as collagen I and collagen III in response to stress as an adaptive mechanism. Additionally, they are responsible for maintaining ECM components by increasing the production of growth factors such as TGF-b (Camelliti, Borg, & Kohl, 2005) which stimulate transcription factor expression for the collagen type I procollagen gene (Chen et al., 1999).

Cellular contractions initiated by the cytoskeletal network, exert forces on the ECM which are essential for tendon healing. However, most of the cellular contraction studies have been conducted on dermal fibroblasts in a wound healing model (Brown, Prajapati, McGrouther,

Yannas, & Eastwood, 1998; Coleman, Tuan, Buckley, Anderson, & Warburton, 1998; Dahlmann-Noor, Martin-Martin, Eastwood, Khaw, & Bailly, 2007; Eastwood, McGrouther, & Brown, 1994; S. Liu et al., 2010). In 1979, Bell and colleagues first reported the production of a tissue-like structure, with contractile fibroblasts seeded in collagen lattice (Bell, Ivarsson, & Merrill, 1979). In tendon, type I collagen is a predominant component of the ECM and is highly conserved between species (Dumitru & Garrett, 1957; Kessler, Rosen, & Levenson, 1960; Marenzana, Wilson-Jones, Mudera, & Brown, 2006; Mudera, Morgan, Cheema, Nazhat, & Brown, 2007) therefore use of type 1 collagen lattices to study tendon mechanobiology has provides a bio-mimetic microenvironment analogous to *in vivo* tissue. In order to replicate *in vivo* maximum strain on tendon before the onset of the characteristic crimp pattern (Butler, Grood, Noyes, & Zernicke, 1978), it is possible to use mechanical overload to deliver precise mechanical forces to the fabricated tissue. Previously, cellular contraction of collagen lattices seeded with dermal fibroblasts has been measured using a custom-built culture force monitor (CFM) (Eastwood et al., 1994). The cellular contraction in response to mechanical overload has been investigated using a tensioning force culture monitor (t-CFM) (Eastwood, McGrouther, & Brown, 1998).

The objective of this study was to use a tissue-engineered 3D model of the tendon, to investigate the response of TF to mechanical load. Particular focus was placed on the cytomechanical contraction profile, the acute response of ECM-related genes and the adaptive morphology of the cells. We hypothesised that 10% cyclic strain would result in a greater cellular mechanical response compared with a statically loaded control, stimulating the mechanisms required for the expression of ECM remodelling genes.

2. MATERIALS AND METHODS

2.1 Tendon tissue isolation and cell culture

Experiment design and ethical approval were obtained from the UCL Institutional Review Board (IRB). All experiments were carried out as per the regulation of Home Office and guidelines of Animals (scientific procedure) Act 1986. New Zealand white rabbits (aged between 16 to 25 weeks, weighing between 3.0 to 4.5 kg) were used to extract tendon fibroblasts. The posterior area of the hind legs was shaved with a clipper and disinfected by iodine solution, to allow for an incision to be made around tibiofibular area to expose the posterior tibial tendon. Extracted tibial tendons were washed with PBS containing 10% antibiotic and antimycotic solution (Sigma-Aldrich, Dorset, UK). The epitendon was removed and the remaining tissue was subsequently digested with 5% collagenase type 1 (Sigma,UK), at 37°C in a water bath for 3 hours. Subsequently, the mixture was filtered through a 70 μm cell strainer to remove undigested ECM. The isolated TF were then cultured in T225cm^2 tissue culture flasks, with growth media (Dulbecco's Modified Eagle Medium [DMEM], Sigma, Irvine, UK), containing 10% fetal calf serum (FCS) (First Link, UK) and 1% Penicillin and Streptomycin (Invitrogen, UK)

2.2 Fabrication of tendon- fibroblast populated collagen lattice

Collagen lattices were cast using 4 ml rat tail collagen type I (First Link, Birmingham, UK) and 500 μl of 10X Minimal Essential Medium (Invitrogen, Paisley, UK), neutralised using 5M and 1M sodium hydroxide (Sigma-Aldrich, Dorset, UK). 500 μl DMEM containing 5×10^6 cells /ml (passage 0), was added to the neutralised solution and poured into plastic molds of $75 \times 25 \times 15$ mm dimensions. Custom built 'A-frames' allowed for collagen attachment and

the application of uniaxial tension. These molds were kept in a CO_2 incubator at 37ºC and 5% CO_2 for 15 minutes to allow for fibrillogenesis, contributing to the fabrication of a tendon fibroblast populated collagen lattice (tFPCL). In this study collagen, acellular gels were fabricated with the same method. However, for the positive control, we have used rabbit's posterior tibial tendon. .

2.3 tFPCL Static load

The tFPCLs were attached to an adapted CFM (Eastwood et al., 1994). One of the stainless-steel frames was connected to the force transducer and another to the fixed point (Fig. 1a) to measure contraction in a single plane. Contraction of the gel initiated by cell-ECM interaction and matrix remodelling pulled the Vyon beams together, and deflection in the Vyon beams was measured using a micro-strain gauge. The reliability and calibration of the instrument was performed by applying the constant force of 50, 100, 500 millinewton (mN) for 24 hours and the output (constant applied tension at each load) was within the expected limit. The signal from strain gauge was converted from analogue to digital, and contraction profile of tFPCL was quantified with readings taken on a strain indicator (Vishay Micro-Measurements, NC, USA) at a frequency of 1Hz over 24 hours.

2.4 tFPCL Cyclic load

The t-CFM is derived from the CFM, where the cyclic load can apply by the addition of a stepper motor (Micromech, Braintree, UK). Each stepper motor was driven by a microstep control panel (Parker Vix 250IM stepper drive, Parker Irwin, USA). The tFPCLs were attached to the t-CFM as illustrated (Fig.1B). The t-CFM was set up and calibrated by attaching a stable

metal rod, whereby force was linear according to given distances of motor movement. The tFPCLs were subjected to 10% strain and cycles were programmed for 15 minutes loading, followed by 15 minutes unloading, (to 0% strain) with a 15-minute time delay in between each loading and unloading cycle, for a total of 24 hours. Acellular gels were used as a control, to allow for the investigation of cell-mediated responses to load.

2.5 Sirius red staining

Post loading, tFPCLs were fixed in 10% formalin (in saline) for one hour and embedded in paraffin wax. Sections of 5 μm were prepared on microscope slides, de-waxed and re-hydrated in series with xylene and ethanol. Sections were then stained with Sirius red [Sirius direct red 80 (Sigma-Aldrich Dorset, UK)] for one hour, followed by two changes of acidified water. Finally, they were de-hydrated in a series of ethanol washes and cleared in xylene. Images were obtained on a light microscope (Olympus BH-2) fitted with an Olympus Camedia 2020 camera. All images were converted to greyscale and analysed by using ImageJ software version 1.49 (NIH, USA). Each image was outlined with a straight line throughout the image and pixel intensities were measured against a region of interest. Calculated pixel intensities were pooled for each condition. The change in the pixel intensities correlated to the collagen distribution and remodelling for each group.

2.6 Cellular alignment under load

The midsections (25mm from the centre) of tFPCL were fixed in 4% formalin saline for 30 minutes and permeabilised in 0.15% triton-X in PBS for 15 minutes. Sections stained using 1.5% phalloidin (Invitrogen, Life Technologies Ltd, Paisley, UK) and 1% DAPI (Vector Labs, Peterborough, UK) and mounted on glass slides with a coverslip. Images were obtained by

using an upright fluorescent microscope Olympus BX61 (Olympus, Tokyo, Japan). Image analysis was conducted using ImageJ software (NIH, USA). Images were adjusted to the highest contrast level to filter out the noise and converted to the binary function, which had divided the image into object and background by using an iso-data algorithm. Images were further analysed by using 'Analyse particle' function, and particle size was set to 100 pixels, which filtered out small non-descript structures from the image. Circularity was set between 0.00 – 0.80 (this needs to be less than 1, as 1 is a perfect circle and angle cannot be determined) and with the outline of the image, the angle was measured for both static and cyclic load conditions. A frequency graph was plotted for each cell angle from 0-180° for both conditions to investigate whether cell alignment was affected.

2.7 Deformation of TF- nuclei under load

To study the deformation of the nucleus and the cytoplasm under static and cyclic load, a 10mm mid-segment of the tFPCL was fixed in 4% formalin saline for 30 minutes. It was then permeabilised in 0.15% triton-X in PBS, stained with 1% phalloidin (Invitrogen, Life Technologies Ltd,Paisley, UK) and 0.5% propidium iodide (PI) (Invitrogen, Life Technologies Ltd,Paisley, UK), after which it was mounted on glass slides and fixed with a coverslip. A Bio-Rad confocal microscope (BIO-RAD Hertfordshire, UK) fitted with an Olympus BX51 upright microscope (Olympus, Tokyo, Japan) was used to image the sections. To perform analysis of the deformation of TF under static and cyclic loading conditions, fluorescence images were imported to ImageJ software (NIH, USA) using the 'spit colour channel' function.

2.8 Gene expression

The tFPCLs were homogenised using a power homogeniser, and RNA was isolated using TRIzol according to the manufacturer's instructions (Invitrogen, Paisley, UK). The cDNA

synthesis was carried out using a Precision nanoscript reverse transcription kit (Primer Design, Southampton, UK). RNA and cDNA yield was quantified by using Nano drop, ND-1000 spectrophotometer (NanoDrop Technologies, Inc. Wilmington, USA). Gene quantification was determined using an ABI 7300 real-time PCR machine (qPCR) (Applied bio-system, UK). Custom designed and synthesised primers were used for qPCR (Table 1) (Primer design, Southampton, UK) and results were analysed as delta-delta ct and expressed as relative quantification (RQ) values, normalised to unloaded tFPCLs and GAPDH as a housekeeping gene.

2.9 Statistical analysis

All experiments were carried out independently for a minimum of three biological replicates (n=3). Statistical analysis was performed using SPSS 21.0. (SPSS IBM cooperation, Chicago, USA). One-way ANOVA and t-test with Post-Hoc analysis by Bonferroni corrections were used to determine differences between conditions. Results are reported as a mean ± standard deviation, where $p < 0.05$ was considered significant.

3. RESULTS

3.1 tFPCL static load

As the isolated cells were passaged for experiments, the effect of passage on the contractile force was investigated (P0, P1, P3, and P6). It was observed that the P0 cells were more contractile as they generated greater maximum force $818 \pm 85.56 \mu N$ in the early hours under static load, compared with all other passages. When gels were seeded with TF at P1, the calculated maximum force was less at $701 \pm 98.23 \mu N$, which continued statistically significant to drop with increasing passage (P3 = $482 \pm 43.87 \mu N$; p= 0.0048 and P6 = $266 \pm 65.89 \mu N$; p=

0.0009) (Fig. 2a and c). In the view of the contractile profile of the TF under different passages, all gels for subsequent mechanical loading experiments were cast with P0 cells. The contraction of TF at P0 was divided into three distinct phases (Fig. 2b); the first phase was between 0 to 4 hours, where force was generated exponentially to 818 ± 76.23 μN. The graph pattern in phase one (0 to 4 hours) was characteristic of cell-matrix attachment, cell motility and traction forces (Eastwood, Porter, Khan, McGrouther, & Brown, 1996). Phase two was between 4 to 20 hours, which consisted of minor increases in contractile forces that resulted in a plateau phase until 20 hours, where force reached 871 ± 87.12 μN. In phase three from 20 to 24 hours, the force output measured was reduced to 823 ± 98.54 μN which may reflect reductions in both cell and matrix tension.

3.2 tFPCL cyclic load

Gels were seeded with 1×10^6 cells/ml at P0 and mounted onto the t-CFM for loading experiments. Following on from the static loading experiments these independent constructs followed a similar pattern, whereby an exponential increase in the net contractile forces (to 830 ± 45.43 μN) was evident in the initial 4 hrs prior to the application of external load. A 10% external strain was then applied on the tFPCLs, which resulted in the exponential increase in the observed force to 4452 ± 213.45 μN. It is important to consider that this increase in force is not cell-mediated and merely a product of the motor driving the strain gauge. When the external load was fixed during the static loading period, the residing TF reduced endogenous force as a potential stress shielding mechanism. This resulted in a decrease in the net contractile force to 4251 ± 348.89 μN. Similarly, when tFPCLs were unloaded, TF decreased net contractile force from 1001 ± 78.43 μN to 936 ± 85.21 μN (Fig. 3a). Hence, it was evident that endogenous matrix tension was maintained by TF in the tFPCLs, by an active cellular response in the

opposing direction of applied force to maintain ECM tension. As cycle number increased (i.e. repeating cycles) there was a change in the recorded peak force during the static phase from 182 ± 45.21 μN at a 1st hour to 31 ± 12.87 μN at the 16th hour (Fig. 3b). In contrast, the difference in the force in control acellular gels was marginal (423 ± 34.21 μN to 80 ± 12.11 μN).

3.3 TF alignment under the force

Investigating cellular alignment following 24 hours of static loading, demonstrated a bipolar and stellate morphology with non-aligned orientation (Fig. 4b). This non-aligned morphology was similar to non- loaded tFPCLs, where the matrix was not uniaxially loaded (Fig. 4a). The greatest cellular response was observed following cyclic loading, whereby all cells were aligned in the direction of the applied force (Fig. 4c). This demonstrates that TF aligns as a physiological response under load, to facilitate maximum force transmission across the tissue. Cellular alignment and distinct morphology were also found in the native tendon, demonstrating the ability of tFPCLs to recapitulate features of *in vivo* tissue. TFs were seen aligned in a single plane located between collagen fibres (Fig. 4d). As described above, under tension TF undergo mechanical adaption with altered cellular alignment and orientation. This alignment was further studied by calculating the cellular angle. In the tFPCLs static angle of cellular alignment was non-uniform from 0º to 180º degrees, however, the tFPCLs subjected to cyclic loading contributed to cellular alignment within a range 110º to 180º and showed a normal distribution (Fig. 4e). This alignment of the cells is based on the principle of strain gradients (i.e. 10%) applied uniaxially and as such the strain on the surrounding matrix resulted in matrix remodelling and cellular alignment.

3.4 Loading effect on the cellular deformation

Cellular deformation studies indicated that in the cyclic condition (Fig. 5c), nuclei were deformed along with the cytoplasm. This demonstrates a further cell response to mechanical load similar to that seen in NT (Fig. 5d). The ratio of the change in the area of the nucleus and cytoplasm was $36.36 \pm 14.47\%$ (Fig. 5e), illustrating the degree to which the cell structure changed in response to load. In the static and unloaded conditions (Fig. 5 a and b) there was no major nucleus or cell membrane deformation seen. The area change in the nucleus and cytoplasm in the static condition was $80.49 \pm 11.05\%$, (no statistical significance) and with this type of morphology, it would be suggested that maximum force transmission across matrix would not be achieved.

3.5 Collagen remodelling

Histological sections of tFPCL in the cyclic condition, (Fig. 6c) were similar to that of the native tendon (Fig. 6d), whereby there was the predominant uptake of the picro-sirius stain. Furthermore, there was evidence that the collagen fibrils were remodelled, oriented and aligned in the direction of the force. It is unlikely that this is as a consequence of neo-collagen synthesis by TF in such a short period of time and should be investigated further. In the static condition (Fig. 6b), there was evidence that fibrils were partially oriented when compared to the non-loaded controls (Fig. 6a). Evidence of cell-mediated remodelling was poor, suggesting that it is cyclic mechanical loading which contributes to this response. Collagen intensity was quantified by using the pixel intensity from the captured images in each condition. The grey values for the tFPCL-cyclic condition was predominant (145 ± 23 pixels) ($P < 0.05$), with lower values observed for static (65 ± 19 pixel) and control (41 ± 5 pixel) conditions, respectively. Analysis for NT demonstrated this measure to be higher (312 ± 37 pixels) (Fig. 6e), suggesting denser collagen structures.

3.6 Gene expression

Relative quantification (RQ) values indicated that all genes were upregulated in tFPCL-cyclic condition, when compared to tFPCL-static controls. Collagen I mRNA (RQ 4.45± 1.02) *(p =<0.0001)* in tFPCL-cyclic was fourfold higher compared to tFPCL-static (RQ 1.8 ± 0.32) and Collagen III mRNA in tFPCL-cyclic (RQ 0.22± 0.04) was one-fold higher than tFPCL-static (RQ 0.12±0.06) *(p =>0.99).* Tenomodulin mRNA in the tFPCL-cyclic condition was highly expressed (RQ 1.2± 0.03) compared to tFPCL-static (RQ 0.24± 0.04) *(p = 0.0972))* and TGF-b was twofold higher expressed in tFPCL-cyclic (RQ 0.55± 0.03) as compared to the tFPL-static (RQ 0.1± 0.02) *(p =0.0204)* (Fig. 7)

4. DISCUSSION

Fibroblast mediated matrix tension has been studied in a wound healing model, to investigate the cellular mechanisms which contribute to repair (Brown et al., 1998; Coleman et al., 1998; Dahlmann-Noor et al., 2007; Eastwood et al., 1994). However, to-date TF mediated matrix tension and the mechanisms which regulate ECM remodelling following mechanical loading in tissue-engineered tendon have not been investigated. In tendon, matrix tension is affected by various factors such as internal (muscle-initiated tension) external (passive joint motion) mechanical loading. It is difficult to study acute cellular responses and adaptation to mechanical loading *in vivo*. To this end, model platforms (such as the CFM and t-CFM) have provided a means to investigate the cytomechanical properties of tissue fabricated *in vitro* (Eastwood et al., 1994).

The CFM, being a highly sensitive method, is an excellent platform to measure the accurate force generated by the TF in the initial cellular attachment and contraction phases when in

tethered tFPCLs. As per our knowledge, this is the first time TF contraction has been reported accurately within the μN range under uniaxial load. The contraction data and profile reported here was found to be similar to the models previously described in fibroblasts and endothelial cells respectively (Eastwood et al., 1994; Kolodney & Wysolmerski, 1992). This demonstrates similarities in the mechanisms of attachment, traction and matrix remodelling profiles of TF when compared to fibroblasts and endothelial cells isolated from different tissues. There was also evidence of minor contraction in control cell-free collagen gels, which we attribute to fibril maturation and binding as previously reported by Wood and Keech (Wood & Keech, 1960). This is an important consideration when investigating the contribution of both cellular and extra-cellular responses to mechanical load.

In this study, the TF cytomechanical profile under static load was divided into three discrete phases, which represent the framework of cell behaviour in the 24 hours examined. In phase one (< 4 hours) rapid force generation (to 818 μN) was evident, likely due to cell attachment and cell elongation. Such a response has been reported to correlate to cell migration processes during wound healing *in vivo (Escamez et al., 2004)*. In phase one, cell attachment and the elongation response also supports the hypothesis proposed by Harris et al., whereby the fibroblast traction is responsible for the morphogenetic rearrangement of an ECM similar to that seen in tendons and organ capsules (Harris, Stopak, & Wild, 1981). The passage number of TF used was also found to produce distinct contraction patterns in phase 1 (Fig 2A), which provides evidence of TF heterogeneity. This supports findings reported by Torry et al., in pulmonary fibroblasts, where adult cells are less contractile due to a characterised anchorage-dependent mechanism when compared to neonatal cells (Torry, Richards, Podor, & Gauldie, 1994).

The second identified phase (4 to 20 hours) demonstrated a plateau, which suggests a steady-state in TF contraction (818 μN to 871 μN). The mechanism required to maintain contraction

is thought to depend on myosin ATPase activation and actin-myosin interaction, which has previously been described in a fibroblast wound contraction model (Levinson, Moyer, Saggers, & Ehrlich, 2004). In the third phase (20 to 24 hours), static contraction decreased at the end of 24 hours with the identification of morphological changes of TF. This is possibly due to release of matrix metalloproteinases (MMP) (Kjaer, 2004) by the TF, which would be necessary for cell migration. MMPs disrupt the surrounding extracellular matrix niche through collagen digestion, as reported by Lambert at al. (Lambert, Soudant, Nusgens, & Lapiere, 1992).

The t-CFM is a mechatronic device which has facilitated the study of TF mechanobiology in collagen matrices quantitatively. The t-CFM was used in the current experiments to investigate the response of TF under 10% mechanical loading corresponding to maximum strain a tendon can take before attending a crimp pattern (J. H. Wang, 2006). Cyclic mechanical loading caused cell-free collagen lattices to stretch under applied load (4380 µN). However, in cell-free collagen lattices, there was no evidence of residual displacement in the 15-minute rest period between each loading and unloading cycle. During this resting period, displacement was linear with a difference of 101 µN, illustrating no significant viscoelastic effect of collagen as described in skin fibroblasts (Delvoye, Wiliquet, Leveque, Nusgens, & Lapiere, 1991). Collagen lattice tension was able to return to original tension after unloading, which indicated that there was no permanent plastic deformation (Eastwood et al., 1998). This is thought to be a consequence of the matrix increasing in stiffness following mechanical loading cycles (anti-thixotropic property of collagen), resulting in a reduced cellular response. Increases in cellular mediated force following a reduction in applied load are thought of as a mechanism to maintain tensional homeostasis. Hence, we can conclude that TF mediated matrix tension reported under loading and unloading, was entirely cell-mediated and we have established a method to calculate TF response during mechanical loading.

Mechanical loading of the tissue generates strain on the TF, initiating cellular contractions and deformation which are essential for tendon healing. These cell generated contractions exert a force on the ECM (Grinnell, 1994), whilst also activating various cellular and molecular mechanisms. Evidence suggests that scar formation is a consequence of steep contraction, whereas, in contrast, minimal contraction can result in impaired tendon healing. Therefore, the optimal strain (10%) is essential for tendon healing. In this study, 10% external strain was applied (reaching a recorded force of 4452 μN) and when the external load was invariant at resting time, then residing TF in tFPCL reduced endogenous force and exerted force in the opposite direction (4251 μN). This acute response is thought to act as a mechanism of tensional homeostasis, where TF apply active stain upon the ECM. Brown et al., and Eastwood et al., described a mechanism of tensional homeostasis in dermal fibroblasts, where the net resultant force was equilibrated due to actin-myosin motor filaments, cytoskeletal elements, and microtubules, which in turn helps in maintaining cellular polarity (Brown et al., 1998; Eastwood et al., 1994). Furthermore, we have demonstrated that TF generates rapid endogenous force to maintain homeostasis in the early hours of the cyclic load when compared to later hours. In contrast, the effect of loading and unloading in a similar model reported no change in the force at the end of a 1st hour of the experiment, with the lattice returning to its original value (Delvoye et al., 1991). This is an indication of the viscoelastic material property, a phenomenon that was not identified in the current experiments.

Following loading, it was apparent that the cell's nucleus was deformed, along with the cytoskeleton. The ratio of the change in the area nucleus and cytoplasm was significant for cyclic (36.36 ± 14.47%) compared to static (80.49 ± 11.05%) demonstrating cell responses to mechanical load. Kopp et al., characterised the role of mechanoreceptors on Schwann cells as similar to that of TF (Kopp, Trachtenberg, & Thompson, 1997) which also have the same receptors that activate various signalling pathways such as G protein, MAPK's, cAMP

pathways and Ca^{2+} influx on loading (M. Liu, Xu, Tanswell, & Post, 1994). This results in the upregulation of transcriptional factors for the genes which are responsible for matrix remodelling and repair. In this study, genes responsible for ECM production, maintenance and remodelling, as well TF proliferation and maturation were all shown to increase. Specifically, tenomodulin is a tendon-specific gene that highly expressed during tendon injuries and is related to TF proliferation and maturation (Docheva, Hunziker, Fassler, & Brandau, 2005) Such increases in gene expression following cyclic loading compared to static loading, is an indication that TF could sense mechanical stress on them and activate mechanisms that contribute to the expression of genes required for matrix remodelling and increasing matrix stiffness. Future work should seek to further characterise the mechano-chemical mechanisms that are activated in TF during loading, in order to provide further understanding as to the regulation of tendon adaptation and injury.

The mechanical forces also lead to cellular and nuclear deformation, biochemical signalling and cellular alignment in the tendon (Arnoczky et al., 2002). The statically loaded condition showed cellular morphologies that were bipolar and stellate, with the non-aligned orientation of the cells. although loading resulted in the stretching of the cells. Cyclic loading resulted in the maximum cellular response with evidence of stark changes in cellular morphology, illustrating a definitive response of the cells structurally to the applied load. Cellular deformation in the tendon is an indication that the TF acutely adapt to the mechanical forces, demonstrating mechanical dynamism (Arnoczky et al., 2002). There are numbers of studies have been performed under uniaxial and biaxial load (Giannopoulos et al., 2018; T. Wang et al., 2018). However, in this study is that we had applied constant static load and cyclic to a collagen lattice mimicking native tendon for 24 hours and monitored force generation in the real-time which had provided us cytomechanical with quantitative cell physiological data and the similarity between tFPCL- static and tFPCL- cyclic is that, in both conditions. In which

cells were able to sense mechanical tension which resulted in the phenomenon called "mechanical adaption" (Brown et al., 1998). The CFM and t-CFM have limitations in recording the force generated in the uniaxial plane, i.e. X plane (± x-axis). Further experiments should seek to investigate cellular force generation by in Y plane (± y-axis) and Z planes (± z-axis) and also applying sub-physiological load (i.e. < 10%) with various gene expression profile such as MMPs and TIMPs will give greater understanding with regards to the role of mechanobiology of tendons in load-bearing models *in vivo.*

This study demonstrates that TF could sense external mechanical stimuli placed on them and adapt their physical and cyotomechanical properties, including activating genes required for ECM remodelling. Such a model provides a suitable test bed for further investigation of the mechanisms which regulate tendon repair in response to mechanical load and may also provide an environment for the pre-clinical study of putative mechanical and pharmacological interventions.

5. ACKNOWLEDGEMENTS

6. CONFLICTS OF INTERST

The authors declare that they have no conflict of interest.

7. REFERENCES

1. Arnoczky, S. P., Lavagnino, M., Whallon, J. H., & Hoonjan, A. (2002). In situ cell nucleus deformation in tendons under tensile load; a morphological analysis using confocal laser microscopy. *J Orthop Res, 20*(1), 29-35. doi:10.1016/s0736-0266(01)00080-8

2. Bell, E., Ivarsson, B., & Merrill, C. (1979). Production of a tissue-like structure by contraction of collagen lattices by human fibroblasts of different proliferative potential in vitro. *Proceedings of the National Academy of Sciences of the United States of America, 76*(3), 1274-1278.

3. Brown, R. A., Prajapati, R., McGrouther, D. A., Yannas, I. V., & Eastwood, M. (1998). Tensional homeostasis in dermal fibroblasts: mechanical responses to mechanical loading in three-dimensional substrates. *J Cell Physiol, 175*(3), 323-332. doi:10.1002/(sici)1097-4652(199806)175:3<323::aid-jcp10>3.0.co;2-6

4. Butler, D. L., Grood, E. S., Noyes, F. R., & Zernicke, R. F. (1978). Biomechanics of ligaments and tendons. *Exerc Sport Sci Rev, 6*, 125-181.

5. Camelliti, P., Borg, T. K., & Kohl, P. (2005). Structural and functional characterisation of cardiac fibroblasts. *Cardiovasc Res, 65*(1), 40-51. doi:10.1016/j.cardiores.2004.08.020

6. Chen, S. J., Yuan, W., Mori, Y., Levenson, A., Trojanowska, M., & Varga, J. (1999). Stimulation of type I collagen transcription in human skin fibroblasts by TGF-beta: involvement of Smad 3. *J Invest Dermatol, 112*(1), 49-57. doi:10.1046/j.1523-1747.1999.00477.x

7. Coleman, C., Tuan, T. L., Buckley, S., Anderson, K. D., & Warburton, D. (1998). Contractility, transforming growth factor-beta, and plasmin in fetal skin fibroblasts: role in scarless wound healing. *Pediatr Res, 43*(3), 403-409. doi:10.1203/00006450-199803000-00016

8. Dahlmann-Noor, A. H., Martin-Martin, B., Eastwood, M., Khaw, P. T., & Bailly, M. (2007). Dynamic protrusive cell behaviour generates force and drives early matrix contraction by fibroblasts. *Exp Cell Res, 313*(20), 4158-4169. doi:10.1016/j.yexcr.2007.07.040

9. Delvoye, P., Wiliquet, P., Leveque, J. L., Nusgens, B. V., & Lapiere, C. M. (1991). Measurement of mechanical forces generated by skin fibroblasts embedded in a three-dimensional collagen gel. *J Invest Dermatol, 97*(5), 898-902.

10. Docheva, D., Hunziker, E. B., Fassler, R., & Brandau, O. (2005). Tenomodulin is necessary for tenocyte proliferation and tendon maturation. *Mol Cell Biol, 25*(2), 699-705. doi:10.1128/mcb.25.2.699-705.2005

11. Dumitru, E. T., & Garrett, R. R. (1957). Solubilization of rat tail tendon collagen. *Arch Biochem Biophys, 66*(1), 245-247.

12. Eastwood, M., McGrouther, D. A., & Brown, R. A. (1994). A culture force monitor for measurement of contraction forces generated in human dermal fibroblast cultures: evidence for cell-matrix mechanical signalling. *Biochim Biophys Acta, 1201*(2), 186-192.

13. Eastwood, M., McGrouther, D. A., & Brown, R. A. (1998). Fibroblast responses to mechanical forces. *Proceedings of the Institution of Mechanical Engineers, Part H: Journal of Engineering in Medicine, 212*(2), 85-92. doi:10.1243/0954411981533854

14. Eastwood, M., Porter, R., Khan, U., McGrouther, G., & Brown, R. (1996). Quantitative analysis of collagen gel contractile forces generated by dermal fibroblasts and the relationship to cell morphology. *J Cell Physiol, 166*(1), 33-42. doi:10.1002/(sici)1097-4652(199601)166:1<33::aid-jcp4>3.0.co;2-h

15. Escamez, M. J., Garcia, M., Larcher, F., Meana, A., Munoz, E., Jorcano, J. L., & Del Rio, M. (2004). An in vivo model of wound healing in genetically modified skin-humanized mice. *J Invest Dermatol, 123*(6), 1182-1191. doi:10.1111/j.0022-202X.2004.23473.x

16. Giannopoulos, A., Svensson, R. B., Heinemeier, K. M., Schjerling, P., Kadler, K. E., Holmes, D. F., . . . Magnusson, S. P. (2018). Cellular homeostatic tension and force transmission measured in human engineered tendon. *Journal of Biomechanics, 78*, 161-165. doi:https://doi.org/10.1016/j.jbiomech.2018.07.032

17. Grinnell, F. (1994). Fibroblasts, myofibroblasts, and wound contraction. *The Journal of Cell Biology, 124*(4), 401-404. doi:10.1083/jcb.124.4.401

18. Harris, A. K., Stopak, D., & Wild, P. (1981). Fibroblast traction as a mechanism for collagen morphogenesis. *Nature, 290*(5803), 249-251.

19. Kessler, A., Rosen, H., & Levenson, S. M. (1960). Chromatographic fractionation of acetic acid-solubilized rat tail tendon collagen. *J Biol Chem, 235*, 989-994.

20. Killian, M. L., Cavinatto, L., Galatz, L. M., & Thomopoulos, S. (2012). The role of mechanobiology in tendon healing. *J Shoulder Elbow Surg, 21*(2), 228-237. doi:10.1016/j.jse.2011.11.002

21. Kjaer, M. (2004). Role of extracellular matrix in adaptation of tendon and skeletal muscle to mechanical loading. *Physiol Rev, 84*(2), 649-698. doi:10.1152/physrev.00031.2003

22. Kolodney, M. S., & Wysolmerski, R. B. (1992). Isometric contraction by fibroblasts and endothelial cells in tissue culture: a quantitative study. *J Cell Biol, 117*(1), 73-82.

23. Kopp, D. M., Trachtenberg, J. T., & Thompson, W. J. (1997). Glial growth factor rescues Schwann cells of mechanoreceptors from denervation-induced apoptosis. *J Neurosci, 17*(17), 6697-6706.

24. Lambert, C. A., Soudant, E. P., Nusgens, B. V., & Lapiere, C. M. (1992). Pretranslational regulation of extracellular matrix macromolecules and collagenase expression in fibroblasts by mechanical forces. *Lab Invest, 66*(4), 444-451.

25. Levinson, H., Moyer, K. E., Saggers, G. C., & Ehrlich, H. P. (2004). Calmodulin-myosin light chain kinase inhibition changes fibroblast-populated collagen lattice contraction, cell migration, focal adhesion formation, and wound contraction. *Wound Repair Regen, 12*(5), 505-511. doi:10.1111/j.1067-1927.2004.012502.x

26. Liu, M., Xu, J., Tanswell, A. K., & Post, M. (1994). Inhibition of mechanical strain-induced fetal rat lung cell proliferation by gadolinium, a stretch-activated channel blocker. *J Cell Physiol, 161*(3), 501-507. doi:10.1002/jcp.1041610313

27. Liu, S., Xu, S. W., Blumbach, K., Eastwood, M., Denton, C. P., Eckes, B., . . . Leask, A. (2010). Expression of integrin beta1 by fibroblasts is required for tissue repair in vivo. *J Cell Sci, 123*(Pt 21), 3674-3682. doi:10.1242/jcs.070672

28. Liu, Y., Ramanath, H. S., & Wang, D. A. (2008). Tendon tissue engineering using scaffold enhancing strategies. *Trends Biotechnol, 26*(4), 201-209. doi:10.1016/j.tibtech.2008.01.003

29. Marenzana, M., Wilson-Jones, N., Mudera, V., & Brown, R. A. (2006). The origins and regulation of tissue tension: identification of collagen tension-fixation process in vitro. *Exp Cell Res, 312*(4), 423-433. doi:10.1016/j.yexcr.2005.11.005

30. Mudera, V., Morgan, M., Cheema, U., Nazhat, S., & Brown, R. (2007). Ultra-rapid engineered collagen constructs tested in an in vivo nursery site. *Journal of Tissue Engineering and Regenerative Medicine, 1*(3), 192-198. doi:doi:10.1002/term.25

31. Murchison, N. D., Price, B. A., Conner, D. A., Keene, D. R., Olson, E. N., Tabin, C. J., & Schweitzer, R. (2007). Regulation of tendon differentiation by scleraxis distinguishes force-transmitting tendons from muscle-anchoring tendons. *Development, 134*(14), 2697-2708. doi:10.1242/dev.001933

32. Thomopoulos, S. (2011). The role of mechanobiology in the attachment of tendon to bone. *IBMS BoneKEy, 8*(6), 271-285.

33. Torry, D. J., Richards, C. D., Podor, T. J., & Gauldie, J. (1994). Anchorage-independent colony growth of pulmonary fibroblasts derived from fibrotic human lung tissue. *J Clin Invest, 93*(4), 1525-1532. doi:10.1172/jci117131

34. Wang, J. H. (2006). Mechanobiology of tendon. *J Biomech, 39*(9), 1563-1582. doi:10.1016/j.jbiomech.2005.05.011

35. Wang, J. H., Guo, Q., & Li, B. (2012). Tendon biomechanics and mechanobiology--a minireview of basic concepts and recent advancements. *J Hand Ther, 25*(2), 133-140; quiz 141. doi:10.1016/j.jht.2011.07.004

36. Wang, T., Chen, P., Zheng, M., Wang, A., Lloyd, D., Leys, T., . . . Zheng, M. H. (2018). In vitro loading models for tendon mechanobiology. *Journal of Orthopaedic Research, 36*(2), 566-575. doi:10.1002/jor.23752

37. Wood, G. C., & Keech, M. K. (1960). The formation of fibrils from collagen solutions 1. The effect of experimental conditions: kinetic and electron-microscope studies. *Biochemical Journal, 75*(3), 588-598.
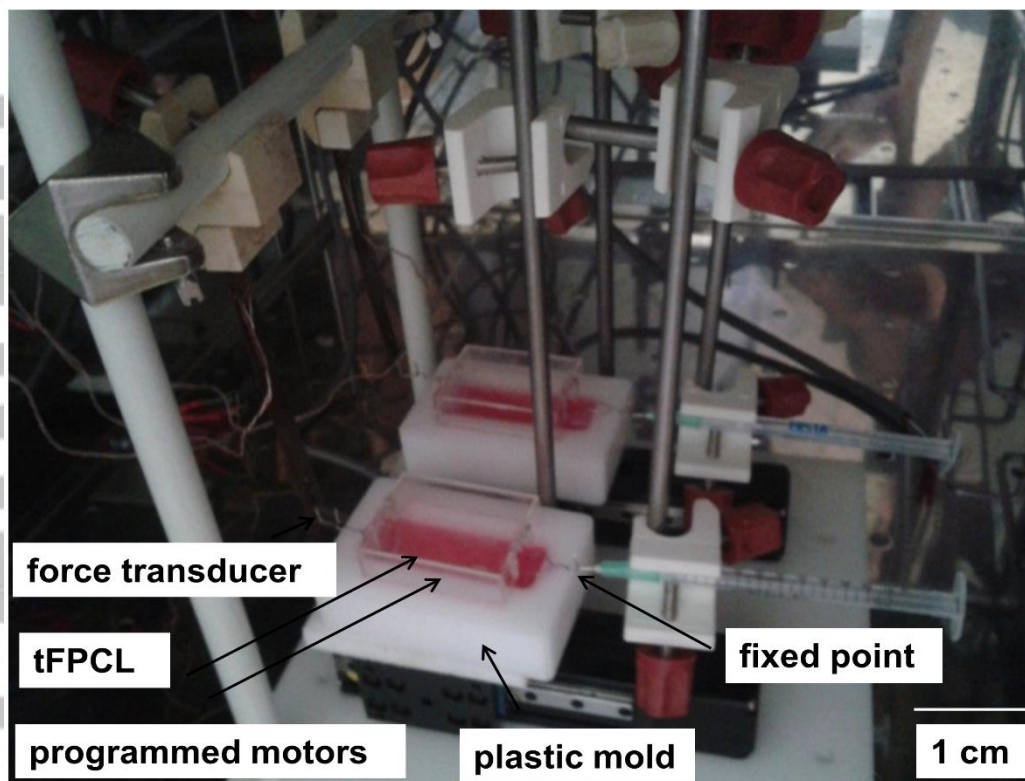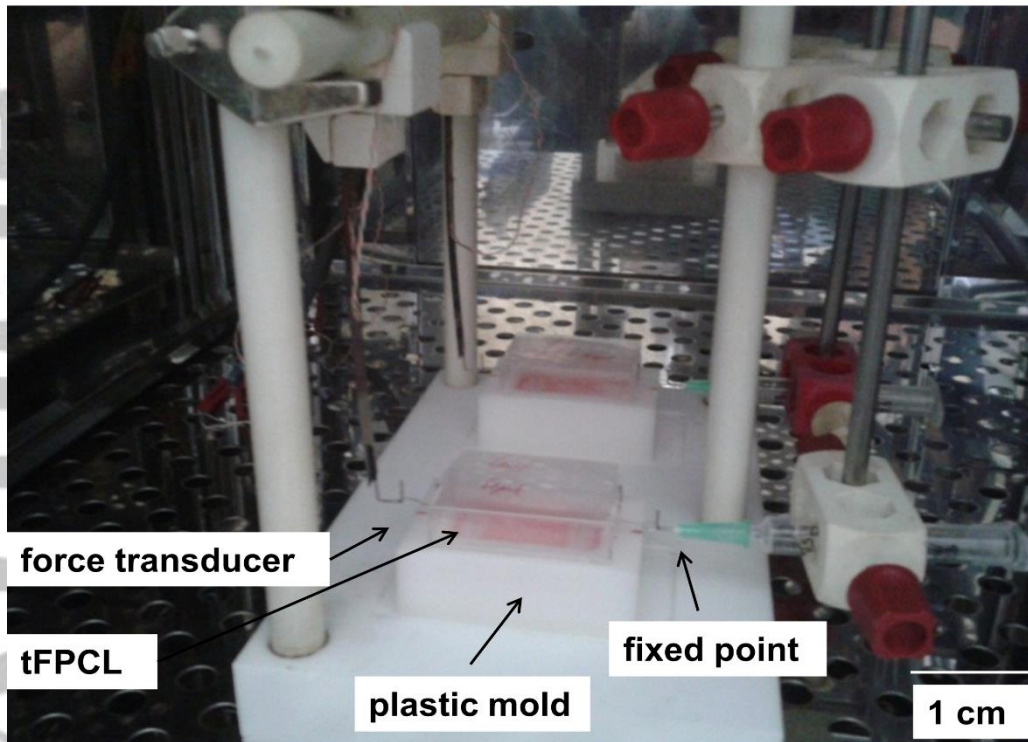
Fig.1. (a) A casted tFPCL inside plastic molds mounted on CFM, adhered to the force transducer and fixed point with stainless steel frame. **(b)** t-CFM set up with tFPCL adhered to the fixed point and force transducer through stainless steel frames and the uniaxial cyclic load was applied.
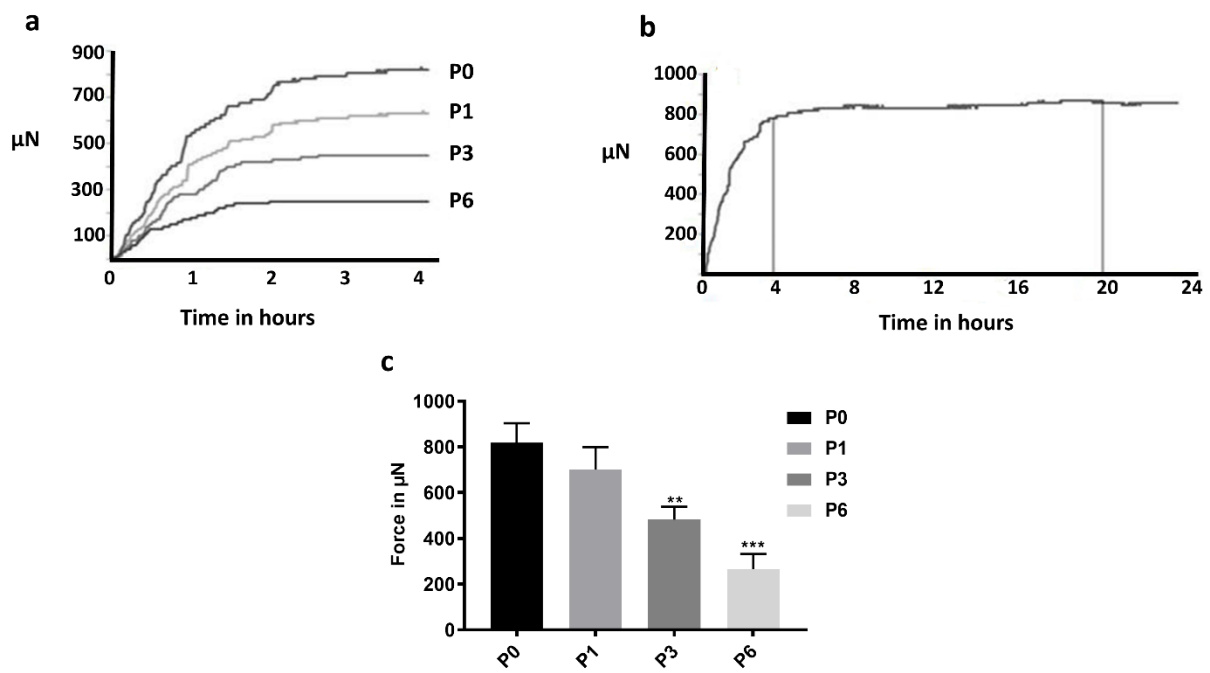
Fig.2. (a) Early contraction force pattern for the for different passage number of TF (P0, P1, P3, and P6). **(b)** Complete contraction profile for tFPCL-static. **(c)** Contraction force the for different passage number of TF.
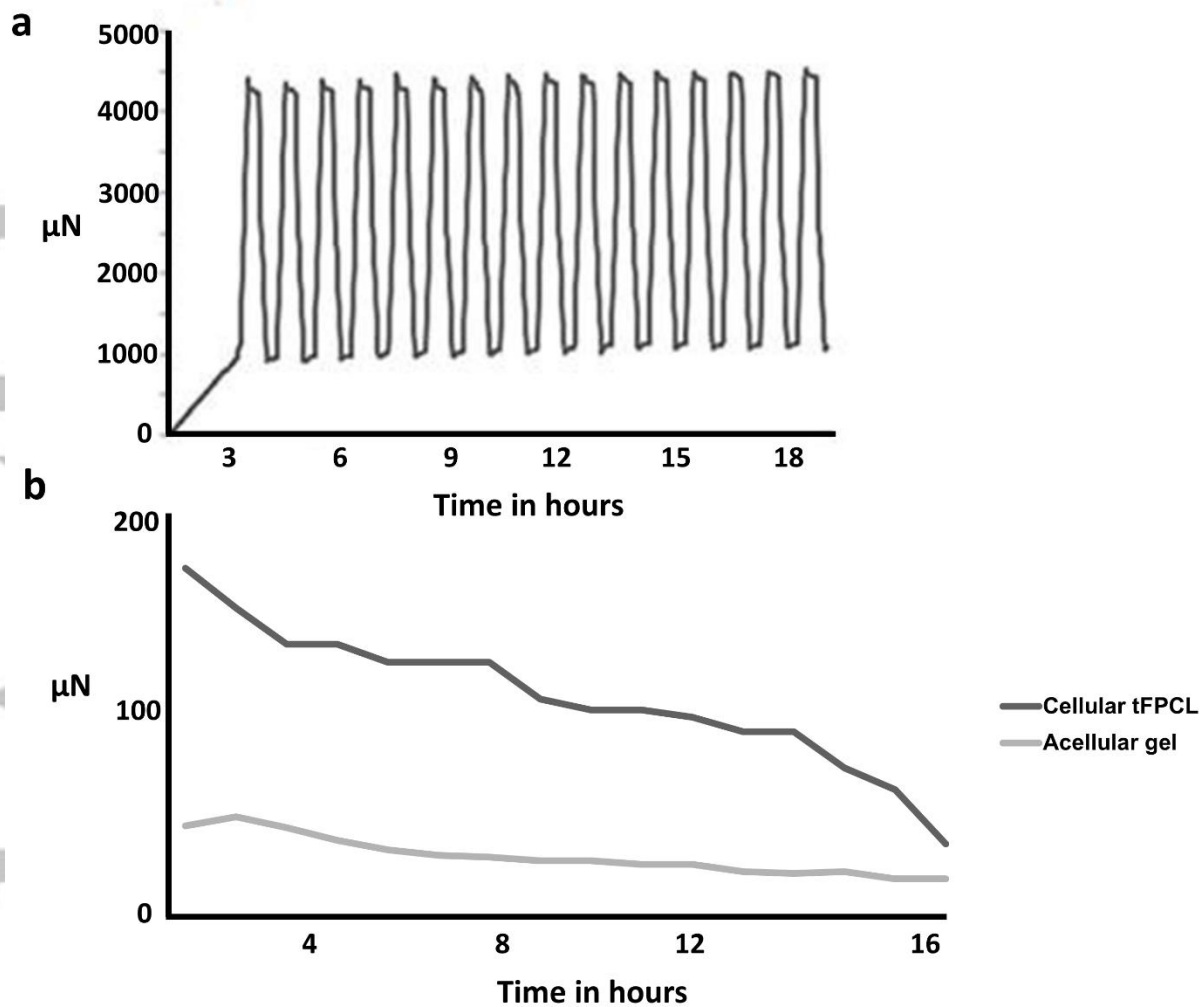
Fig.3. (a) Contraction profile under cyclic load **(b)** The change in the peak force during the resting period for tFPCL-cyclic.
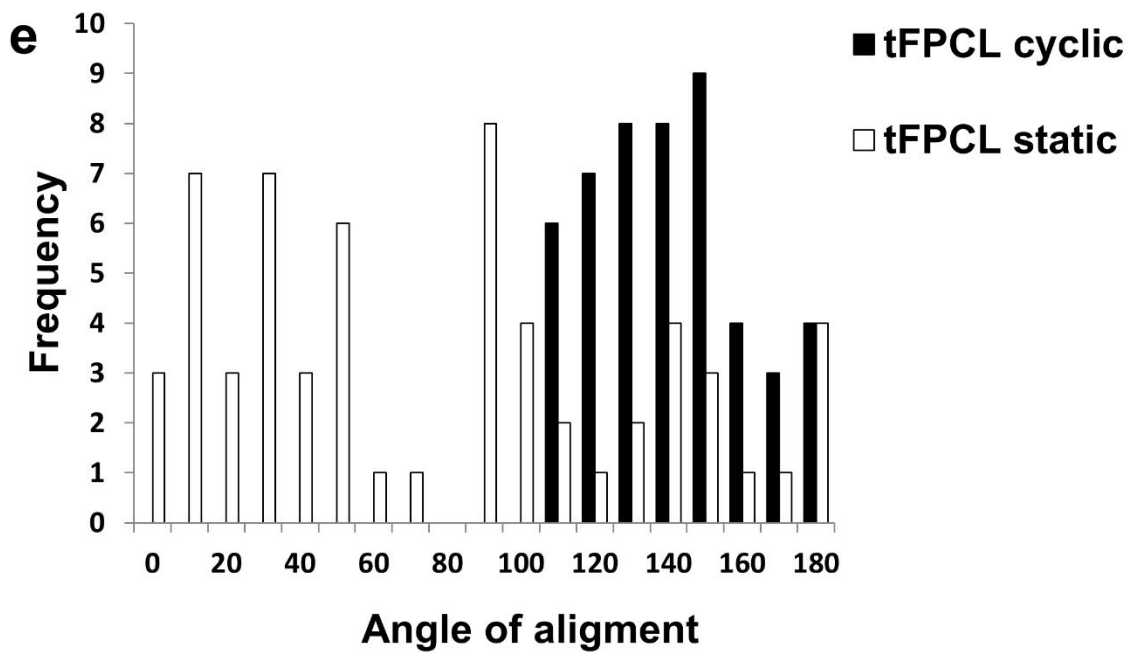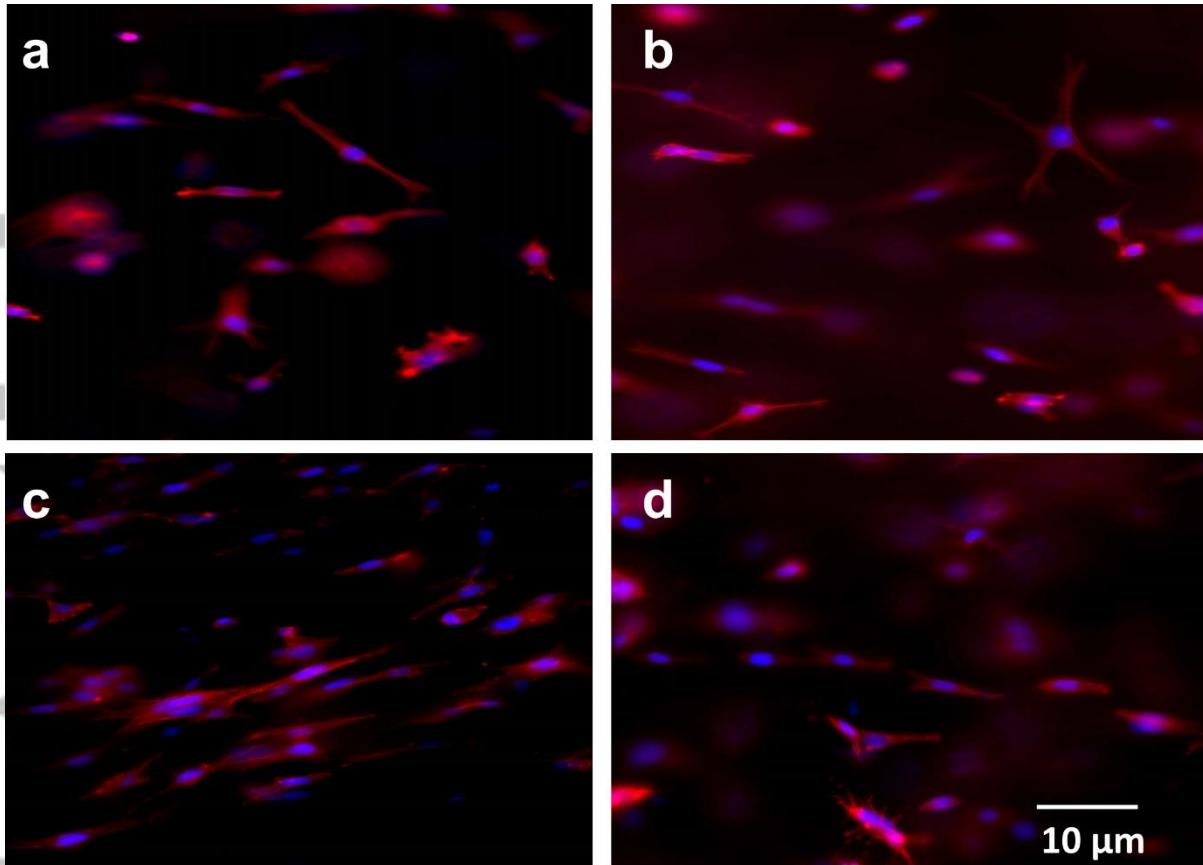
Fig.4. Cellular alignment (a) Unloaded tFPCL (b) tFPCL- static (c) tFPCL-cyclic (d) native tendon (e) Angle of orientation of the tFPCL static and tFPCL cyclic.
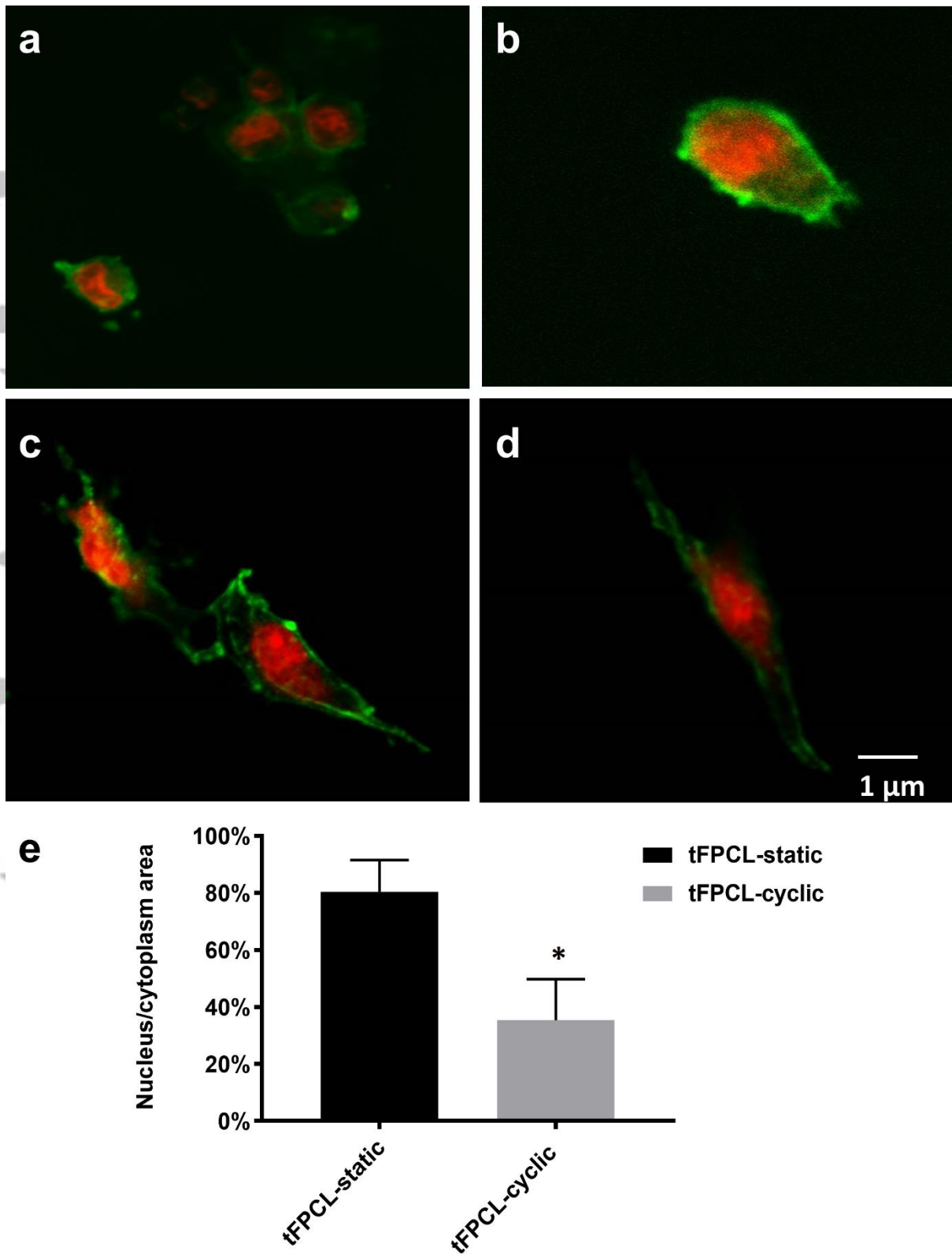
Fig. 5. Cellular deformation (a) unloaded tFPCL. **(b)** tFPCL-static. **(c)** tFPCL-cyclic. **(d)** native tendon. **(e)** change in the area of the nucleus to the cytoplasm of the tFPCL under static and cyclic load after 24 hours of loading *(*denotes the statistical significance of P<0.05).*
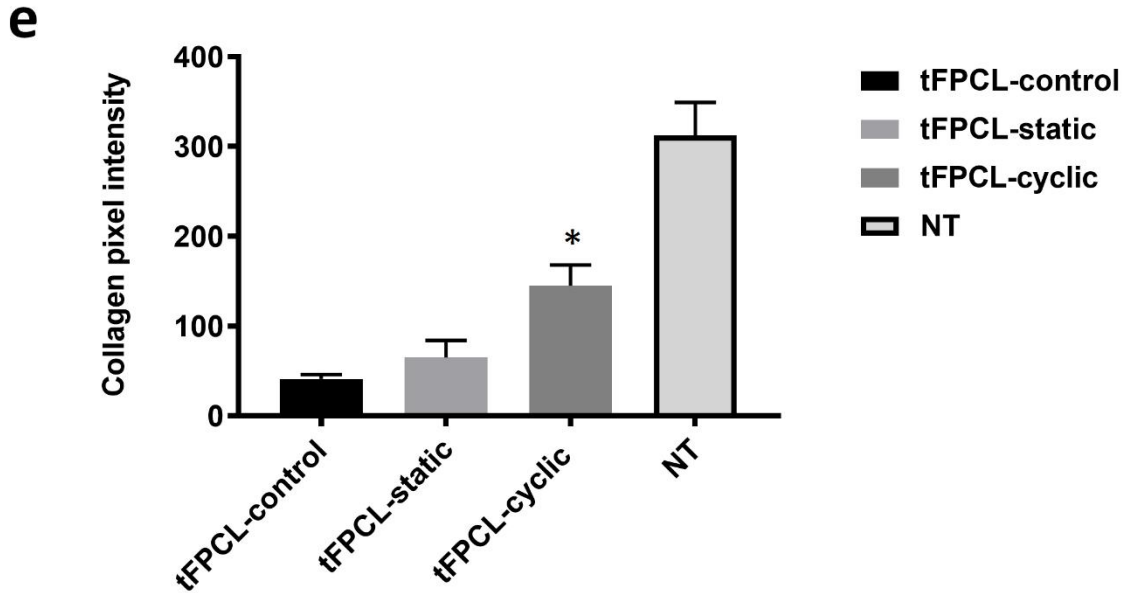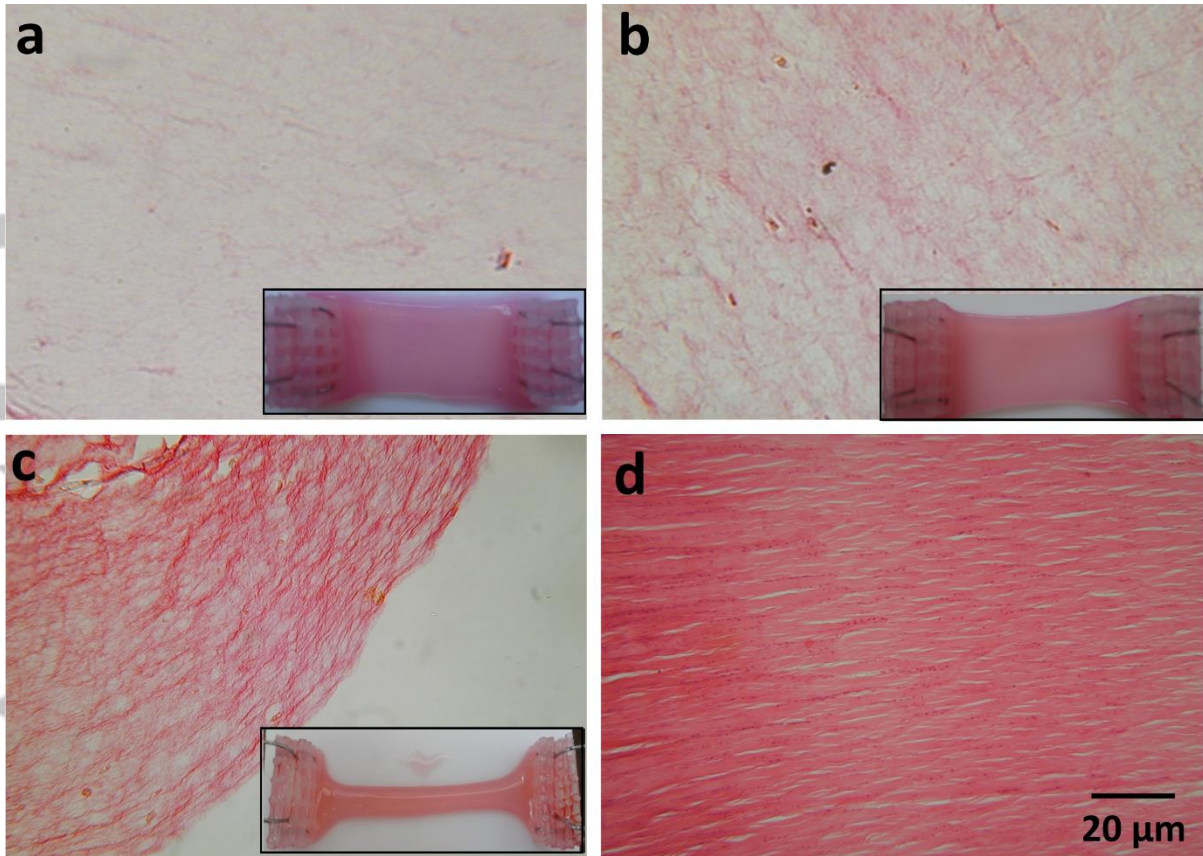
Fig. 6. Collagen remodelling a) unloaded tFPCL. **(b)** tFPCL-static. **(c)** tFPCL-cyclic. **(d)** native tendon. **(e)** Showing collagen pixel intensity for tFPCLs and NT. Lower right corner showing gels after loading *(*denotes the statistical significance of P<0.05).*
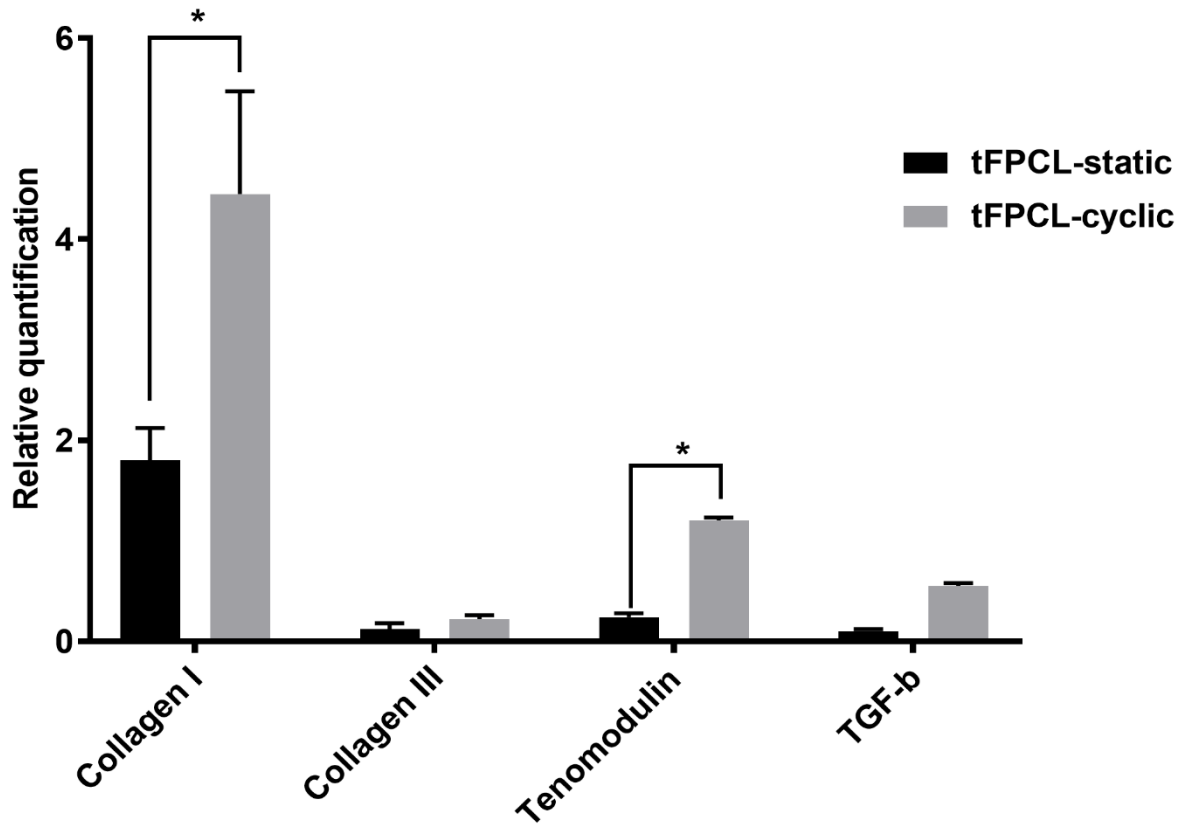
Fig.7. Gene expression profile of the tendon specific genes Collagen I, Collagen III, Tenomodulin and TGF-b after 72 hours under static and cyclic load *(*denotes the statistical significance of P<0.05)*.

Table 1: Forward and reverse primers.

Name of gene	Accession number	Forward Primer	Reverse Primer
Collagen 1A1	XM_017348831.1	5'GGAAACGATGGTGCTACTGG3'	5'CCGACAGCTCCAGGGAAG3'
Collagen type III	XM_002712333.3	5'TAAACGCCAATCCTCTGAGTAT3'	5'AAACTGAAAACCGCCATCCAT3'
Tenomodulin	HM028637	5'ATCTTCTTGGAGGAGACTGTATATG3'	5'AAAGCCTGTCAGCAATTTATCT3'
TGF-b1	XM_00272231	5'CAACGCCATCTATGAGAAAACC3'	5'AAGCCCTGTATTCCGTCTCC3'
GAPDH	NM_001082253	5'CGAGCTGAACGGGAAAC3'	5'CCTGGTCCTCGGTGTAG3'